Electronic Supplementary Information

Electrochemically addressable nanofluidic devices based on PET nanochannels modified with electropolymerized poly-*o*-aminophenol films

Gregorio Laucirica,[1] Vanina M. Cayón,[1] Yamili Toum Terrones,[1] M. Lorena Cortez,[1] María Eugenia Toimil-Molares,[2] Christina Trutmann,[2,3] Waldemar A. Marmisollé[1,*] and Omar Azzaroni[1,*]

[1]Instituto de Investigaciones Fisicoquímicas Teóricas y Aplicadas (INIFTA), Departamento de Química, Facultad de Ciencias Exactas, Universidad Nacional de La Plata, CONICET – CC 16 Suc. 4, 1900 La Plata, Argentina

[2]GSI Helmholtzzentrum für Schwerionenforschung, 64291 Darmstadt, Germany

[3]Technische Universität Darmstadt, Materialwissenschaft, 64287 Darmstadt, Germany

E-mail: wmarmi@inifta.unlp.edu.ar (W.A.M.)

E-mail: azzaroni@inifta.unlp.edu.ar (O.A.)

Base and tip diameter characterization

The base diameter was estimated by scanning electron microscopy (SEM) (**Figure S1(a)**). For this aim, an irradiated multi-pore foil (~2.2 GeV; fluence= 10^7 ions per cm^2) was etched under the same etching conditions that the single-pore. By means of SEM images, a base diameter of 650 ± 50 nm was estimated (N=50).

The tip diameter was determined by the iontronic output in a single-pore PET foil coated with Au (PET/Au). Additionally, the tip diameter after the modification with POAP (PET/Au/POAP) was approximated. With these purposes, channel *I-V curves* were recorded after different electropolymerization cycles. Using a high electrolyte concentration (1 M KCl) is possible discarding surface effects and, therefore, the response can be attributed to geometrical parameters and electrolyte properties.[1] Hence, the tip radius (r_t) was estimated using the equation introduced by Apel *et. al.* (**Equation S1**),[2]

$$R = \frac{1}{\pi\kappa}\int_0^L \frac{dx}{\left[r_B - (r_B - r_t)\exp(-x/h)\right]^2} \qquad \text{(S1)}$$

Where R is the channel resistance at low transmembrane voltages, κ is the specific solution conductance at 25 °C, r_B is the base radius and the parameter h (~500 nm) is a value related to the bullet geometry curvature and was taken from bibliography.[3]

In this way, tip diameter was 80 nm for PET/Au and 30 nm for PET/Au/POAP after 75 cycles of electropolymerization (**Figure S1(b)**). These results indicate a tip size decrease. This fact was studied in previous work.[4]

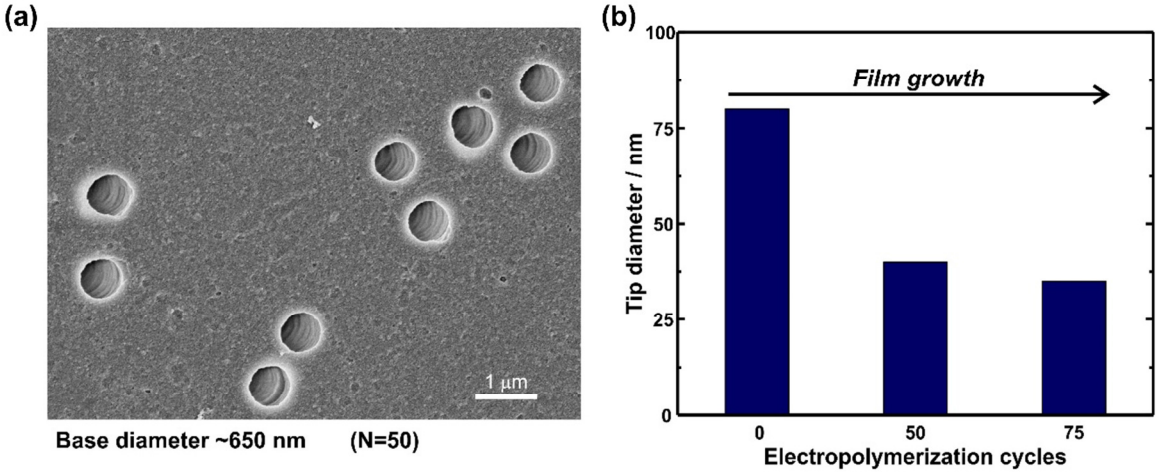

Figure S1. (a) Base channel SEM image. (b) Relation between estimated tip diameter and electropolymerization cycles.

Film properties

Electrochemical characterization

POAP was characterized by electrochemical measurements on Au electrodes using a Gamry Reference 600 potentiostat. Au electrodes were created by sputtering on glass substrates and were treated with soft basic piranha prior to use. The setup consisted of a classical three-electrode array. The reference electrode and the counter-electrode were Ag/AgCl (3 M KCl) and Pt wire, respectively.

For this aim, *o-AP* in an Au electrode was electropolymerized under the same conditions as the Au-coated membranes. Then, the POAP redox behavior was studied by cyclic voltammetry measurements (CV) at different scan rates (**Figure S2**). The voltammetric curve recorded at low scan rate reveals only one redox reaction with $E^{0'}$ in the region around 100 mV (**Figure S2 (a)**). Moreover, currents increased as the scan rate incremented. The relation between the peak current flux (j_p) and the scan rate (<25 mV s^{-1}) is linear as predicted for redox coupled confined with reversible behavior (**Figure S2 (b)**).[5] However, when the scan rate is better than 25 mV s^{-1}, the dependence is linear with its square root as predicted for diffusion-controlled charge-transport process.[6,7]

For its part, the peak potential for the anodic reaction ($E_{p,\ anodic}$) did not show great variations with the scan rate increment (**Figure S2 (c)**). Nevertheless, the peak potential for the reduction reaction ($E_{p,\ reduction}$) varied with the sweeping potential which is attributed to kinetic dependent processes.[8]

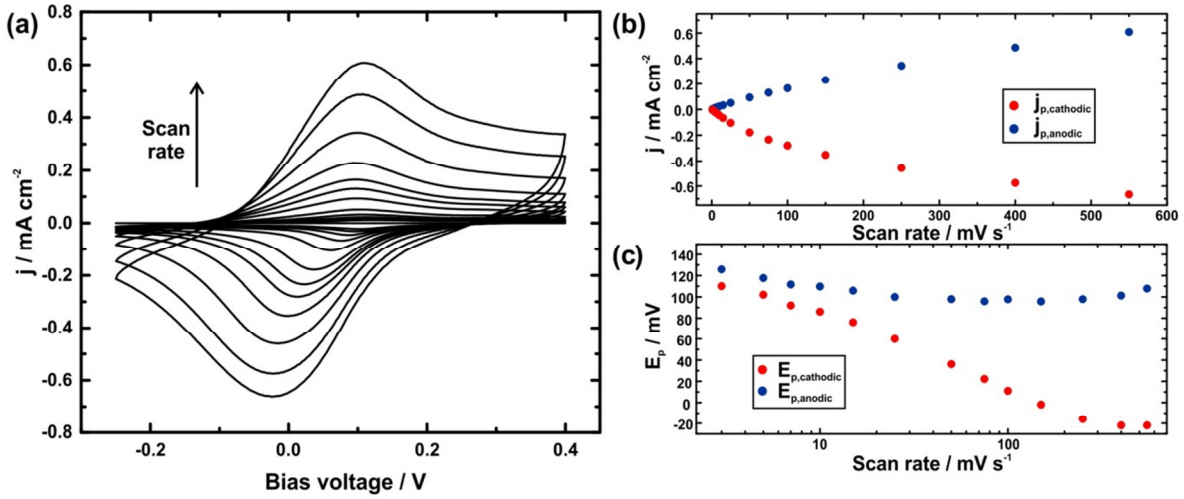

Figure S2. (a) POAP Cyclic voltammetry in Au electrode for different scan rates. (b) Peak current flux and (c) peak potential at different scan rates.

Cell configuration

In order to control both the ionic transport across the nanochannel and, simultaneously, the POAP redox state a bipotentiostat set-up was used. In this regard, were used two potentiostats (*Gamry Reference 600*) connected to different electrode arrangements (**Figure S3 (a)**). A potentiostat was connected to a classical three-electrode array which consisted in a Pt wire (counter-electrode $-CE_1-$), a Ag/AgCl (reference $-R_1-$) electrode and a copper ring that by means of the contact with the Au coating operated as working electrode (W_1) (**Figure S3 (b)**). This arrangement allowed the POAP electropolymerization on the tip side and the film charge state control via the application of a bias voltage. It is important to clarify that the bias voltage applied was referred as gate voltage (V_g) due to its analogy with a field-effect transistor. The other potentiostat was used for recording the ionic transport across the channel by means of a four-electrode array: two Pt wires (working $-W_2-$ and counter-electrode $-CE_2-$) and two Ag/AgCl (working sense $-WS_2-$ and reference $-R_2-$) electrodes (**Figure S3 (c)**). With this arrangement the iontronic response can be related to variations into the nanochannel.[9]

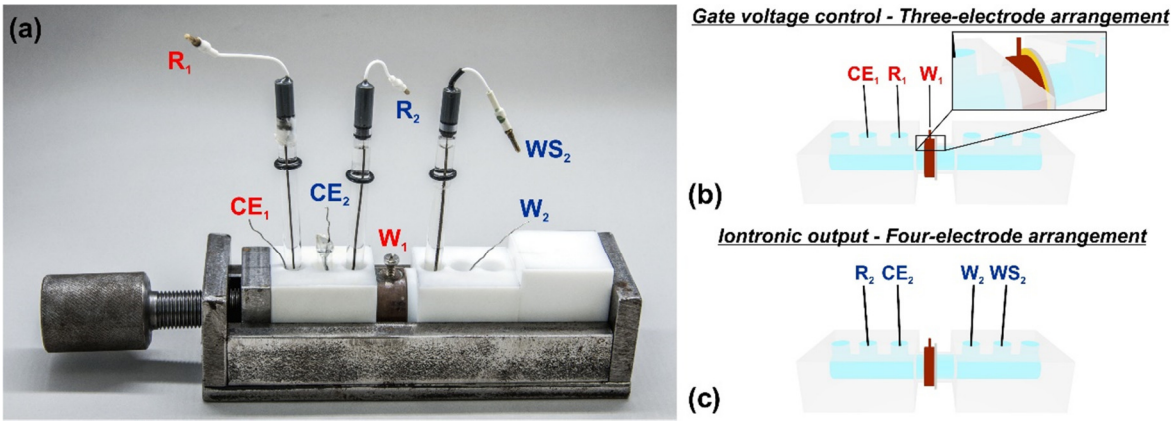

Figure S3. (a) Photograph of home-made cell used for the nFET measurement. Arrangements used for (b) voltage gate control and (c) recording the iontronic output, respectively. Zoom-in shows the contact between the Au coating and the copper ring.

Control experiments

Appropriate control experiment to prove our hypothesis that ionic transport switching is induced for the POAP presence was carried out. For this, *I-V curves* applying different V_g in an Au-coated nanochannel without POAP were performed. The iontronic output did not show significant changes between the curves recorded at V_g= -0.2 V and V_g= 0.2 V (**Figure S4)**. On the other hand, the POAP modified-membrane presents clear variations on the applied gate voltage, showing the coupling of the electroactive polymer layers provides the electrochemical responsiveness.

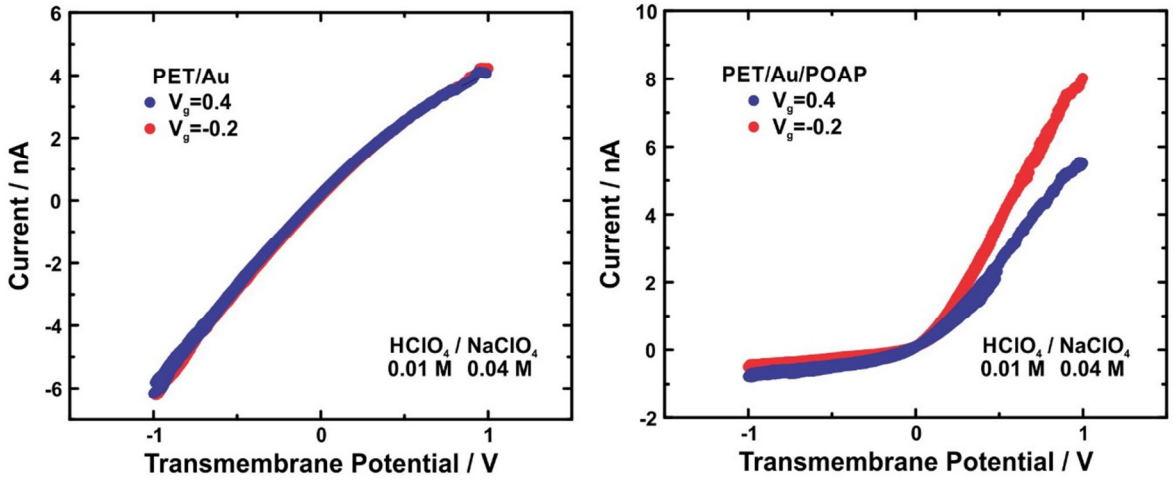

Figure S4. (a) Iontronic output at different V_g for a nanochannel before (left) and after (right) the POAP modification.

On the other hand, **Figure S5** exhibits the different cycles recorded in a classic measurement of ionic transport in nanochannels for the PET/Au/POAP system. The graph shows good current stability as is swept the transmembrane potential.

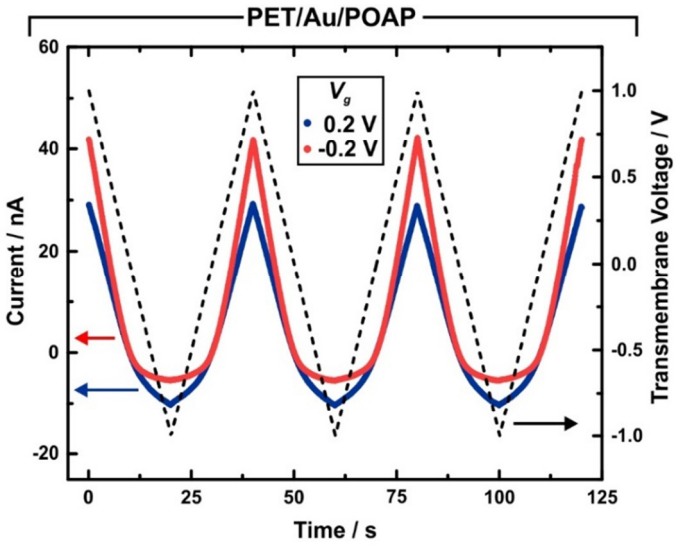

Figure S5. Conductimetric measurements expressed in terms of time. Dashed black line indicates the variation in the transmembrane voltage applied.

POAP acid-base behavior

To asses the acid-base behavior of the reduced form of POAP, *I-V curves* at different pH values in the acidic range were acquired while keeping the V_g at -0.2V to assure the reduced state. Results in terms of the rectification factors are presented in **Figure S6**. Taking into account that the rectification factors can be employed as a measure of the surface charge density, the analysis in terms of the f_{rec} allows estimating the effective p*Ka* value for the $POAP_{(red)}$ form. The sigmoidal fitting in **Figure S6** yields a value of 2.4 for this p*Ka* from the inflection point. This value is in great agreement with previously estimated values by other authors.[6,8,10]

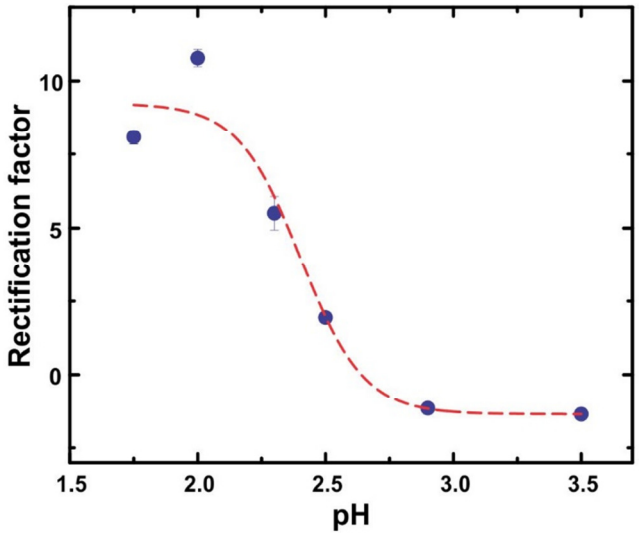

Figure S6. Rectification factor values as a function of the solution pH for a PET/Au/POAP single-channel membrane. *I-V curves* were acquired using a perchlorate concentration of 0.05 M, *i.e.* $HClO_4$ + $NaClO_4$=0.05 M.

Dependence of the contact angle on V_g

The contact angle values of the Au/POAP system under different gate voltages was investigated using an *ad-hoc* set-up (**Figure S7A**). For this aim, drops of 0.01 M $HClO_4$ + 0.04 M $NaClO_4$ solution were deposited on the surface of a plane Au electrode previously modified with POAP in the same conditions as those employed for the nanochannel membranes. The gate voltage was then controlled by a classical system of three-electrodes in contact with the drop. The successful connection between the electrode system and the drop was checked by recording the cyclic voltammetry (**Figure S7B**).

Values of 50° ± 2° and 49°± 3° were obtained for V_g= 0.4 V and -0.2 V respectively. In all cases, the values reported corresponded to the average of five independent measurements. Thus, the change of V_g does not generate appreciable changes in the contact angle (**Figure S7C and D**).

On the other side, the contact angle was measured using a solution drop of 0.01 M $HClO_4$ + 0.04 M $NaClO_4$ + 6.10^{-3} M ascorbic acid (AA). The presence of AA produces a chemical reduction of POAP. However, the contact angle measurements did not show any variation as compared with the oxidized redox form within the experimental error (not shown).

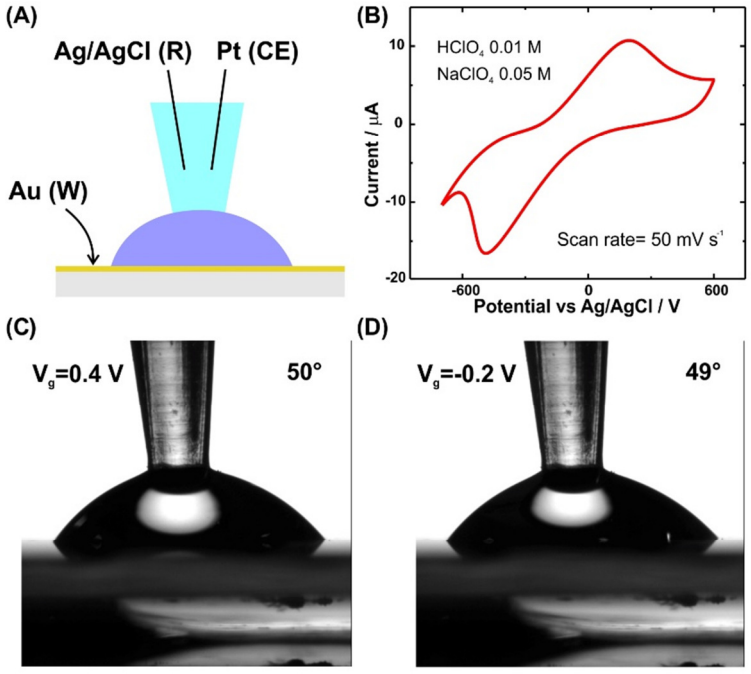

Figure S7. (A) A*d-hoc* set up used to determine the contact angle at different gate voltages. **(B)** Cyclic voltammetry obtained with the three-electrode arrangement in contact with the drop. **(C)** and **(D)** contact angle images for V_g of 0.4 and -0.2 V, respectively.

In summary, the measurements for determining the influence of the oxidation state on the constact angle by both electrochemical and chemical methods did not show appreciable variations between the reduced and oxidized forms or POAP films.

References

1 R. B. Schoch and P. Renaud, *Appl. Phys. Lett.*, 2005, **86**, 1–3.

2 P. Y. Apel, I. V. Blonskaya, N. V. Levkovich and O. L. Orelovich, *Pet. Chem.*, 2011, **51**, 555–567.

3 G. Pérez-Mitta, W. A. Marmisollé, A. G. Albesa, M. E. Toimil-Molares, C. Trautmann and O. Azzaroni, *Small*, 2018, **1702131**, 1–8.

4 G. Pérez-Mitta, W. A. Marmisollé, C. Trautmann, M. E. Toimil-Molares and O. Azzaroni, *J. Am. Chem. Soc.*, 2015, **137**, 15382–15385.

5 A. J. Bard and L. R. Faulkner, *Electrochemical Methods. Fundamentals and Applications*, Wiley, USA, 2nd edn., 2001.

6 R. Tucceri, *Poly(o-aminophenol) Film Electrodes: Synthesis, Transport Properties and Practical Applications*, Springer International Publishing, 1st Editio., 2013.

7 G. Inzelt, *Conducting Polymers: A New Era in Electrochemistry*, Springer-Verlag Berlin Heidelberg, 2008.

8 C. Barbero, J. J. Silber and L. Sereno, *J. Electroanal. Chem. Interfacial Electrochem.*, 1990, **291**, 81–101.

9 Gamry Instruments, 2013.

10 M. E. Carbone, R. Ciriello, S. Granafei, A. Guerrieri and A. M. Salvi, *Electrochim. Acta*, 2015, **176**, 926–940.